A LED Driver With Switched Capacitor

Esio Eloi dos Santos Filho, *Student Member, IEEE*, Pedro H. A. Miranda, Edilson M. Sá, Jr., and Fernando L. M. Antunes

***Abstract*—This paper proposes a switched capacitor-based converter to drive high-power light-emitting diodes (LEDs). In contrast to conventional constant current dc drivers, the current pulse is provided by a switched capacitor. The proposed approach differs from the traditional switched-capacitor-based one, because it uses a small inductor to improve the switching behavior of the converter. Based on the charge control analysis, the effects of switching devices on the proposed converter are evidenced and evaluated. A 6 W, 24 V laboratory prototype has been implemented, while experimental results are presented and discussed to demonstrate the technical feasibility of the proposed converter applied as LED driver.**

***Index Terms*—DC/DC converter, light emitting diodes (LEDs), switched capacitor.**

Nomenclature

DCM	Discontinuous conduction mode.
LED	Light-emitting diode.
SC	Switched capacitor.
ZCS	Zero-current Switching.
ZVS	Zero-voltage Switching.

I. Introduction

THE International Energy Agency (IEA) estimates that about 19% of global electricity demand is used in lighting applications. This statement points toward the need to develop lighting systems with reduced cost and with low environmental impact, thus minimizing energy consumption.

Significant effort has been made toward the replacement of inefficient incandescent light bulbs for more efficient solutions. With the fast development of LED- related technology, commonly used light sources e.g., fluorescent lamps have been increasingly replaced by LEDs. Currently, LED-based lights have a luminous efficacy that makes them competitive with compact fluorescents bulbs, also associated to long useful life and low maintenance. With the increasing concern about energy saving, solid-state lighting based on LEDs has become quite attractive as an efficient light source for general lighting applications [1].

Recently, switched capacitor dc-dc converters have received significant attention from researchers [1]. The increasing popularity of traditional SC converters, also known as charge pumps, is related to their unique characteristics i.e., they employ only switches and capacitors, while the energy transfer is achieved by controlling the charging and discharging process of the capacitors. SC converters have the advantages of light weight, small size, and high power density. An overall analysis of SC converters related to energy efficiency can be seen in [2]–[9]. The conventional understanding is that losses in SC converters are mainly caused by intrinsic resistances and hard switching of semiconductor devices. However, the controversial proposal in [7] claims that the increase of the switching frequency and capacitance values can enhance the efficiency of SC converters. SC converters are often applied in low power applications, while connected in parallel at higher power levels.

The study presented in [10] proposes a 2 W frequency modulated SC converter to drive LEDs. However, the average current is directly proportional to the difference between the supply voltage and the LED forward voltage. It is known that the rated LED forward voltage may vary, what affects the LED array. Besides, the forward voltage also depends on the LED junction temperature, making this proposal inadequate for open-loop operation.

This paper presents a SC converter supplied by 24 V dc source. Unlike conventional SC converters, the proposed converter uses a small additional magnetic component so that the power delivered to the LEDs does not depend on the forward voltage, thus improving the converter efficiency. This issue can be achieved by increasing the on time of the SC, what reduces the peak currents through the circuit.

Considering that the input voltage is constant, the converter does not need a closed loop control system. It is able to operate under soft switching condition e.g., ZCS, allowing the switch to operate at high frequency, with consequent reduction of size and cost if compared with other LED drivers.

II. Proposed Converter

Fig. 1 shows the basic circuit of the proposed SC topology, which is a half-bridge converter. Considering one switching period, capacitor C_s is charged and discharged. The energy stored in the capacitor is transferred to the load and switches S_1 and S_2 operate complementarily.

Inductance L_o is very small, with consequent reduction of cost and higher efficiency. The converter operates in DCM,

Manuscript received October 15, 2013; revised December 18, 2013 and January 17, 2014; accepted January 23, 2014. Date of publication February 26, 2014; date of current version September 16, 2014. Paper 2013-ILDC-630.R2, presented at the 2012 IEEE/IAS International Conference on Industry Applications, Fortaleza, Brazil, November 5–7, and approved for publication in the IEEE TRANSACTIONS ON INDUSTRY APPLICATIONS by the Industrial Lighting and Display Committee of the IEEE Industry Applications Society. This work was supported by the following Brazilian research financing agencies: FINEP, CNP, and FUNCAP.

E. Eloi dos Santos Filho and F. L. M. Antunes are with the Department of Electrical Engineering, Federal University of Ceará (UFC), Fortaleza 60455-76, Brazil (e-mail: esioeloi@gmail.com; fantunes@dee.ufc.br).

P. H. A. Miranda is with the Federal Institute of Ceará (IFCE), Fortaleza 60020-181, Brazil (e-mail: pedromiranda@gmail.com).

E. M. Sá, Jr. is with the Federal University of Ceará (IFCE), Fortaleza 60020-181, Brazil (e-mail: edilson.mineiro@gmail.com).

Color versions of one or more of the figures in this paper are available online at http://ieeexplore.ieee.org.

Digital Object Identifier 10.1109/TIA.2014.2308397

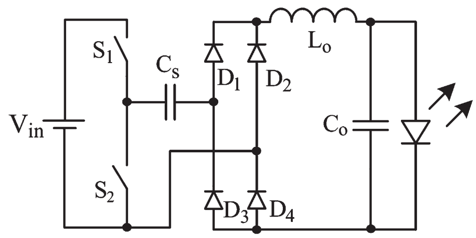

Fig. 1. Basic circuit of the proposed converter.

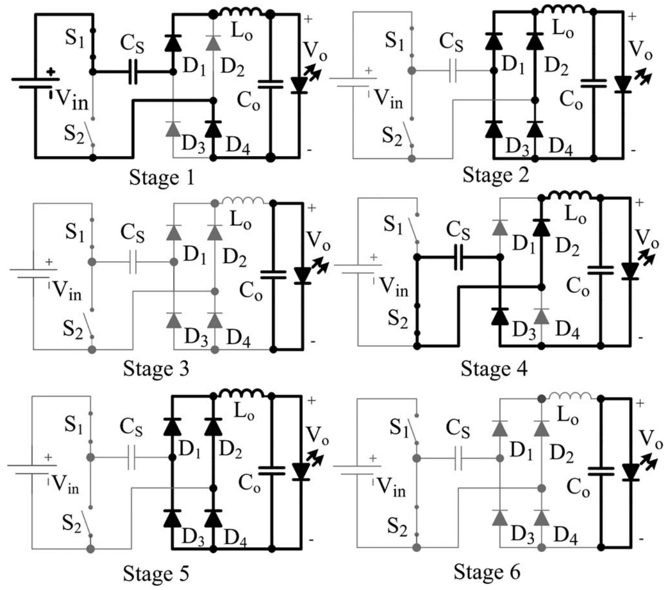

Fig. 2. Operating stages of the proposed converter.

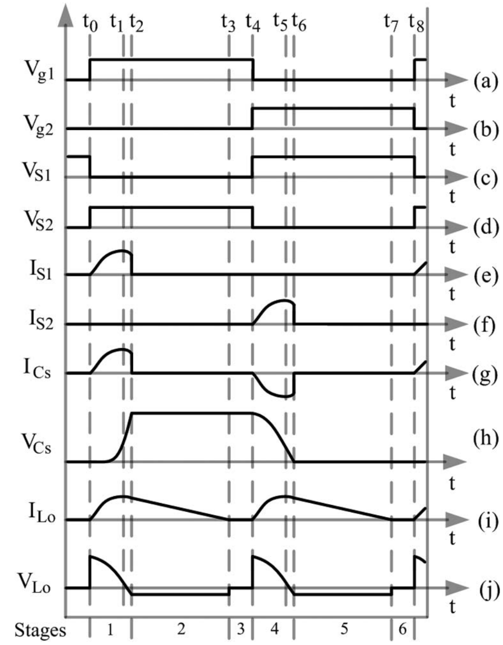

Fig. 3. Main theoretical waveforms of the proposed converter.

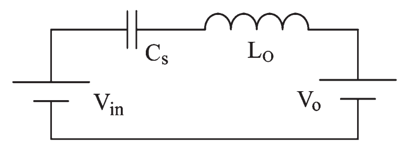

Fig. 4. Simplified representation of the first stage.

where the inductor stores energy during part of the switching period and later on it is completely transferred to the load. Inductor L_o is added to allow the full charging ($V_{Cs} = V_{\rm in}$) and discharging of switched capacitor C_s. Since the LED forward voltage does not affect the charging and discharging process of C_s, the power delivered to the load does not depend on the output voltage V_o.

The DCM operation of the inductor allows obtaining ZCS of the ideal switches S_1 and S_2. Since C_s capacitor is fully charged and discharged, switches S_1 and S_2 are turned off with zero current. Therefore, the converter operates with negligible switching losses, thus enabling high frequency operation and increased efficiency.

To simplify the quantitative and qualitative analyses of the proposed converter, some assumptions must be made. Switches S_1 and S_2 operate in a complementary way and with duty cycle of 0.5. Filter capacitor C_o is large enough to ensure the voltage source characteristic imposed by LEDs. The converter operation can be divided in six stages, which are shown in Fig. 2.

Stage 1 $(\boldsymbol{t_0 - t_2})$-At instant t_0, the voltage across C_s capacitor is null. Besides, switch S_2 is turned off and switch S_1 is turned on. The voltage across C_s increases until it reaches the input voltage ($V_{\rm in}$). At instant $t = t_2$, the current through capacitor C_s becomes zero. At t_1, the peak current flows through capacitor C_s.

Stage 2 $(\boldsymbol{t_2 - t_3})$-During this stage, the remaining energy stored in L_o flows through the diodes and such current decreases linearly to zero at $t = t_3$. Since the diodes are considered as ideal, all four devices remain turned on in Fig. 2.

Stage 3 $(\boldsymbol{t_3 - t_4})$-During this stage, capacitor C_o provides energy to the LED. At $t = t_3$, half the energy provided by the input source is transferred to the load represented by the LED and C_o. Within the same time, the remaining half is stored in the switched capacitor C_s.

Stage 4 $(\boldsymbol{t_4 - t_6})$-At t_4, the voltage across C_s is equal to $V_{\rm in}$. Besides, switch S_1 is turned off and switch S_2 is turned on. During the time interval corresponding to this stage, the whole energy stored in capacitor C_s is transferred to the load. At $t = t_5$, the peak current flows through capacitor C_s. At $t = t_6$, the voltage across C_s is null.

Stage 5 $(\boldsymbol{t_6 - t_7})$-This stage is similar to the second one and the same conditions are valid in this case.

Stage 6 $(\boldsymbol{t_7 - t_8})$-This stage is similar to the third one and the same conditions are valid in this case.

Fig. 3 shows the main theoretical waveforms. All switches are turned on at null current i.e., under ZCS condition.

During the first stage, the converter can be represented by the LC circuit shown in Fig. 4. At $t_0 = 0$, switch S_1 is turned on and both the voltage across switched capacitor C_s and the current through inductor L_o are null.

The resonance angular frequency for simplified circuit in Fig. 4 is defined by

$$\omega_o = \sqrt{\frac{1}{L_o.C_s}}. \tag{1}$$

The voltage across switched capacitor C_s as a function of time during the first stage is given by

$$V_{C_S}(t) = -(V_{\text{in}} - V_o)\cos(\omega_o \cdot t) + (V_{\text{in}} - V_o). \tag{2}$$

The current through inductor L_o during the first stage is given by $i_L(t)$ as

$$i_L(t) = \sqrt{\frac{C_s}{L_o}} \cdot (V_{\text{in}} - V_o)\sin(\omega_o \cdot t). \tag{3}$$

At the end of the first stage 1 $(t = t_2)$, the voltage across the switched capacitor is equal to the input voltage V_{in}. Thus, by manipulation (2), expression (4) can be obtained

$$V_{C_S}(t_2) = V_{\text{in}} = -(V_{\text{in}} - V_o)\cos(\omega_o \cdot t_2) + (V_{\text{in}} - V_o). \tag{4}$$

By isolating t_2 in (4), expression (5) results

$$t_2 = \sqrt{L_o \cdot C_s}\arccos\left(\frac{V_o}{V_o - V_{\text{in}}}\right). \tag{5}$$

Considering that only real values of x are valid in (6), and also substituting (5) in (3), (7) is obtained, which defines the current through inductor L_o at the end of the first stage $(t = t_2)$

$$\sin(\arccos(x)) = \sqrt{1 - x^2} \tag{6}$$

$$i_L(t_2) = \sqrt{\frac{C_s}{L_o}} \cdot \sqrt{V_{\text{in}}^2 - 2 \cdot V_{\text{in}} \cdot V_o}. \tag{7}$$

For the complete charging of switched capacitor C_s with the input voltage V_{in}, the current through inductor L_o at the end of the first stage must not be zero. Thus the condition stated in (8) must be obeyed

$$\sqrt{\frac{C_s}{L_o}} \cdot \sqrt{V_{\text{in}}^2 - 2 \cdot V_{\text{in}} \cdot V_o} > 0. \tag{8}$$

The condition given in (9) is determined from (8), which must be satisfied for the accurate converter operation as described before

$$V_o < \frac{V_{\text{in}}}{2}. \tag{9}$$

Since the current across inductor L_o decreases linearly at during the second stage, and by using boundary conditions, (10) is obtained

$$-V_o = L_o \cdot \frac{di}{dt} = L_o \cdot \frac{-i_L(t_2)}{\Delta t_2} \tag{10}$$

where Δt_2 is the time interval that defines the second stage $(t_3 - t_2)$.

By isolating the time interval corresponding to the second stage in (10), expression (11) results

$$\Delta t_2 = \frac{1}{\omega_o} \cdot \sqrt{\frac{V_{\text{in}}^2}{V_o^2} - \frac{2 \cdot V_{\text{in}}}{V_o}}. \tag{11}$$

If a commercial integrated circuit (IC) e.g., IR2153 is used to drive the switches in a half-bridge, the dead time of the component must be also considered. In this case, the dead time T_{td} is given by

$$T_{td} < \Delta t_2 + \Delta t_3 \tag{12}$$

where Δt_3 is the time interval corresponding to the third stage 3 $(t_4 - t_3)$.

A half switching period $(T/2)$ can be defined by

$$\frac{T}{2} = t_2 + \Delta t_2 + \Delta t_3. \tag{13}$$

Substituting (12) in (13) gives (14) as a function of the switching frequency (f_s)

$$\frac{1}{2 \cdot f_s} > t_2 + T_{td}. \tag{14}$$

Substituting (5) in (14) gives L_o as

$$L_o < \frac{\left(\frac{1}{2 \cdot f_s} - T_{td}\right)^2}{C_s \cdot \left[\arccos\left(\frac{V_o}{V_o - V_{\text{in}}}\right)\right]^2}. \tag{15}$$

The rms current through the circuit can be proportionally reduced according to the value of L_o, because the amount of energy stored in L_o increases and the peak current is reduced. Hence, considering a tolerance of 10% for components L_o and C_s, (15) can be written as

$$L_o = \frac{\left(\frac{1}{2 \cdot f_s} - T_{td}\right)^2}{1,25 \cdot C_s \cdot \left[\arccos\left(\frac{V_o}{V_o - V_{\text{in}}}\right)\right]^2}. \tag{16}$$

At the beginning of the fourth stage $(t = t_4)$, the energy stored in switched capacitor C_s can be given by

$$E_{C_s}(t_3) = \frac{1}{2} \cdot C_s \cdot V_{\text{in}}^2 \tag{17}$$

where $E_{C_s}(t_4)$ is the stored energy in C_s at $t = t_4$.

The energy stored in the switched capacitor at $t = t_4$ is transferred to the LED array during half of the switching period of the controlled switches. Therefore, the average power transferred to the output represented by P_o, which corresponds to the very power of the LED array, can be determined by (18) from (17)

$$P_{out} = E_{C_s}(t_4) \cdot 2 \cdot f_c \cdot \eta \tag{18}$$

where η is the converter efficiency.

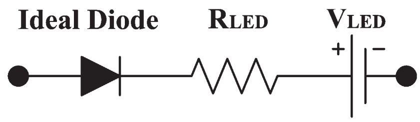

Fig. 5. Simplified electrical model of the LED.

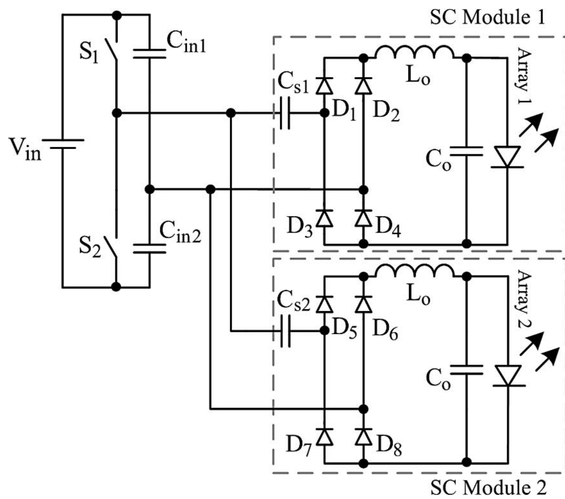

Fig. 6. Proposed converter with two LED arrays.

Substituting (17) in (18) gives (19) as

$$P_{out} = C_s \cdot f_c \cdot \eta \cdot V_{\text{in}}^2. \tag{19}$$

A power LED can be represented by the simplified electrical model shown in Fig. 5 [11]. The LED intrinsic series resistance R_{LED} is due to the current diffusion in the semiconductor and the device is designed for a low value of R_{LED} to minimize losses. Thus, it can be stated that the LED presents an inherent behavior of voltage source. The aforementioned model is considered to simulate the circuit proposed in this paper.

Traditional SC converters are typically designed for relatively low power levels. If more power is needed, a simple solution lies in the connection of several SC modules in parallel, as shown in Fig. 6.

Individual LEDs have slightly different forward voltages. This difference can compromise the current sharing among the arrays. Several actives and passives techniques have been used to reduce the current sharing issue [1], [12]–[25]. Active methods use active devices and usually a control circuit to implement a current regulator connected in series with the LED array [15]. The use of linear current regulators often leads to the reduction of the circuit efficiency at low power applications. On the other hand, the use of switched current regulators provides higher efficiency when compared to the aforementioned approach, although cost is increased. The use of passive methods using passive components such as capacitors or coupled inductors to achieve good current sharing may cause the cost to be reduced. However, when coupled inductors are used, an appreciable number of magnetic components is usually necessary. The passive approach based on capacitors often requires a sinusoidal source with high peak value, while its impedance must be high to ensure good current sharing among LED arrays [13], [26].

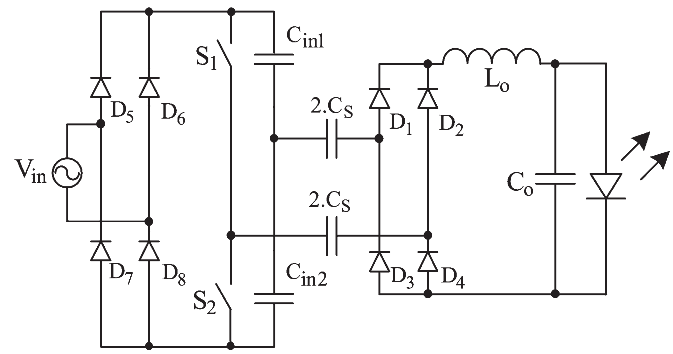

Fig. 7. Proposed converter with isolation capacitor.

The proposed converter can be used to improve current sharing, because it does not depend on the LED forward voltage. Thus, the current is equally distributed among the LEDs, because the forward voltages have similar magnitude. Moreover, each circuit has an independent switched capacitor, which limits the current through the load. Besides, if an output circuit is damaged, the remaining ones will operate correctly, thus ensuring constant current to the load. Therefore, the converter does not require the feedback of the LED array to stabilize the current or compensate its operation when one or more arrays are disconnected. Several switched capacitor modules can be connected in parallel, each one supplying a LED array, as long as the rated output power limit of the half-bridge inverter is respected.

The proposed converter can also be isolated by an alternative method as shown in Fig. 7. In this case, the switched capacitors are used as isolation capacitors, although special devices are needed for this purpose, e.g., dual safety capacitors (Y-cap) [15], [27]–[29].

III. Power Control and Switched Capacitor

The control of the LED current is performed by the SC, which is a prominent advantage of the circuit. The SC is responsible for limiting the power transferred to the LEDs. Thus, the average output current is directly proportional to the switching frequency, considering that the input voltage is constant. Therefore, closed loop operation is not necessary to regulate the LED current.

Expression (19) shows that the power transferred to LED array does not dependent on the voltage across it (V_o). Since the proposed converter operates under ZCS condition independently on the time intervals of the third and sixth stages, the switching frequency can be decreased to reduce the power applied to LED array, as the frequency can be modulated to compensate for variations of the input voltage. Thus, the luminous intensity of the LED array can be adjusted by frequency modulation of the converter. Since the value of C_s is constant and the converter efficiency can be considered constant as an initial approach, the power transferred to LED array can be estimated from the input voltage (V_{in}) and the switching frequency of the inverter. Therefore, the converter does not require current sensors to stabilize the power applied to LED

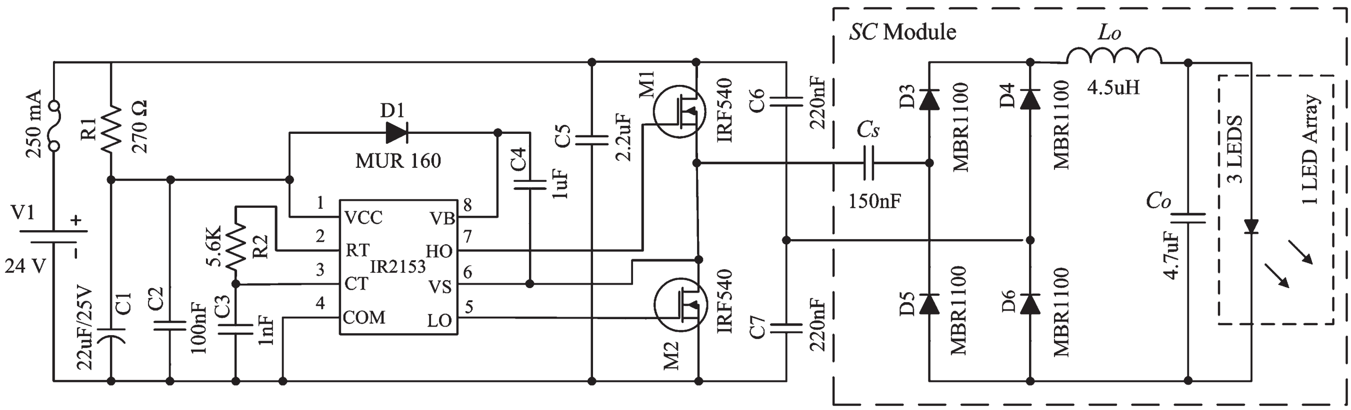

Fig. 8. Complete schematic of proposed SC converter.

array, which leads to a simpler implementation, reduced cost, and reduced dimensions.

The power applied to the LED array can be defined by (20) by multiplying the current average value (I_{AVG}) and the output voltage (V_o). Thus, as the output power is stabilized and voltage variation across the LED array is low, the LED array current variation is also reduced

$$P_{out} = I_{AVG} \cdot V_o. \tag{20}$$

Isolating the value of capacitance C_s in (19) and substituting it in (20), (21) is determined

$$C_s = \frac{I_{AVG} \cdot V_o}{f_s \cdot \eta \cdot V_{\text{in}}^2}. \tag{21}$$

The LED array voltage, which is the output voltage of the converter, can be determined by

$$V_o = n \cdot (V_{\text{LED}} + R_{\text{LED}} \cdot I_{AVG}) \tag{22}$$

where n is the number of LEDs in series in the array.

IV. Design Consideration

The proposed circuit was implemented experimentally validated by using the schematic shown in Fig. 8. The converter was thoroughly evaluated using an input controlled source regulated at 24 V. IC IR2153 is used to drive switches M1 and M2, which consist of typical MOSFETs IRF540. The intrinsic oscillator circuit of IR2153 was set at a switching frequency of 130 kHz, which allows the reduction of magnetic components and capacitors. C_3 is a polyester capacitor used to minimize the frequency variation with the temperature.

Three white LEDs Luxeon III Emitter LXHL-PW09 are used as load. From the voltage versus current characteristic provided by the LED manufacturer, the intrinsic resistance $(R_{\text{LED}} = 0.9\ \Omega)$ and the LED forward voltage $(V_{\text{LED}} = 3.15\ \text{V})$ can be determined. Thus, the LED array output voltage is according to (23), where $n = 3$ and the rated current is 0.9 A

$$V_o = 3 \times (3.15 + 0.9 \times 0.9) = 11.88\ \text{V}. \tag{23}$$

Filter capacitor C_o is calculated from (24), which is given in [11]. To determine C_o, a ripple current $(\Delta I_{LED\%})$ of 10% is considered

$$C_o = \frac{2}{3 \cdot \Delta I_{LED\%} \cdot (2 \cdot \pi \cdot f_s) \cdot (n \cdot R_{\text{LED}})} = 3.03\ \text{uF}. \tag{24}$$

In this case, the commercial value of 4.7 μF has been chosen for the polypropylene capacitors due to their low series resistance and long useful time. The output power is then calculated using (20) as

$$P_{out} = I_{AVG} \cdot V_o = 0.9 \times 11.88 = 10.69\ \text{W}. \tag{25}$$

For an input voltage of 24 V, IC IR2153 is supplied through a 270 Ω resistor to limit the current through the IC. At low power, as in the case of the proposed converter, the power consumption of the driver circuits may correspond to a considerable portion of the overall losses. Components R_2 and C_3 are responsible for defining the switching frequency. In the output rectifier bridge, four Schottky diodes MBR 1100 are used due to the high frequency operation. The design of the SC and the filter inductor is performed by using (26) and (27), respectively. The SC capacitance (C_s) is calculated from (21) as

$$C_s = \frac{I_{AVG} \cdot V_o}{f_s \cdot \eta \cdot V_{\text{in}}^2} = \frac{0.9 \times 11.88}{130 \times 10^3 \times 0.95 \times 24^2} = 150.3\ \text{nF}. \tag{26}$$

The commercial value of 150 nF is adopted for the switched capacitor. Inductance L_o is calculated by (27), where the dead time of IC IR2153 is 1.2 μs

$$L_o = \frac{\left(\frac{1}{2 \times 130 \times 10^6} - 1.2 \times 10^{-6}\right)^2}{1,25 \times 150 \times 10^{-9} \cdot \left[\arccos\left(\frac{11.88}{11.88 - 24}\right)\right]^2} \cong 4.5\ \text{uH}. \tag{27}$$

Hence, $L_o = 4.5\ \mu$H is assumed. For the physical implementation of the inductor, cores CNF are used, which does not need a reel, what reduces the final cost of the magnetic component. Table I shows the designed components and specifications. Table II shows the specifications for inductor L_o.

TABLE I
DESIGN CONSIDERATIONS AND PARAMETERS SET

Parameter	Value
Switching Frequency (f_s)	130 kHz
Switched Capacitor (C_s)	150 *n*F
Inductance (L_o)	4.5 µH
Output Filter Capacitance (C_o)	4.7 µF
Ripple Current through the LED (ΔI_{LED})	10%
Output Power (P_{OUT})	10.69 W

TABLE II
SPECIFICATIONS OF INDUCTOR L_o

Parameter	Value
Indutance (L_o)	4.5 µH
Operation frequency (f_s)	130 kHz
Core (Thorton IP12R)	CNF 7
Used Wire	AWG 29
Number of turns (N_{Lo})	12
Number of wires in paralell	4

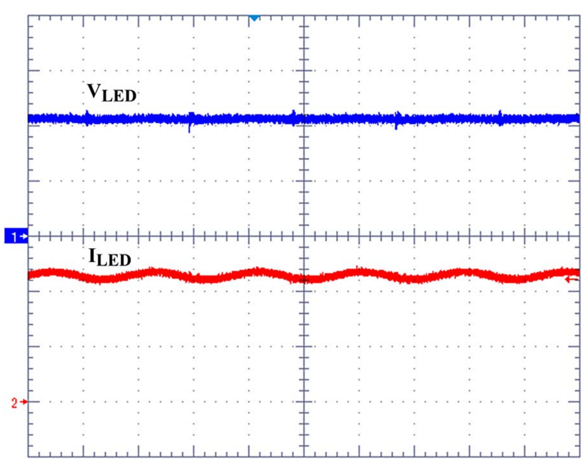

Fig. 9. Voltage (CH1) and current (CH2) waveforms in Led array (Ch1: 5 V/div., 2 μs/div.; Ch2: 200 mA/div., 2 μs/div.).

V. EXPERIMENTAL RESULTS

Fig. 9 shows the voltage across and the current through the LED array. The average current through LED is 457.4 mA and the average voltage is 10.62 V, resulting in 4.85 W.

Fig. 10 shows the voltage across and the current through switch M_2. The current peaks occur due to discharge of intrinsic capacitances of MOSFETs. When the switch is turned on under zero current, the drain-to-source voltage is not null and the energy stored in the intrinsic capacitance is dissipated in the semiconductor increasing switching losses. The losses due the MOSFET capacitances can be determined by [30]. The total measured switching loss in both switches is about 1.5 W.

Conventional MOSFETs have high value intrinsic capacitances, which cause high current peaks during the switching transition, as shown in Fig. 10. In this case, more efficient MOSFET switches with low effective capacitance or even IGBTs are recommended, which are more suitable to achieve ZCS operation and allow the reduction of turn-on switching losses, thus improving the converter performance. Also, is possible add a magnetic element i.e., a transformer, to improve the switching operation. It is then possible to achieve ZVS operation by using the intrinsic capacitance and intrinsic diode of the MOSFET associated with the transformer magnetizing inductance, as presented in [31] and [32], even though the addition of the magnetic element cause size, volume, and weight of the converter to increase.

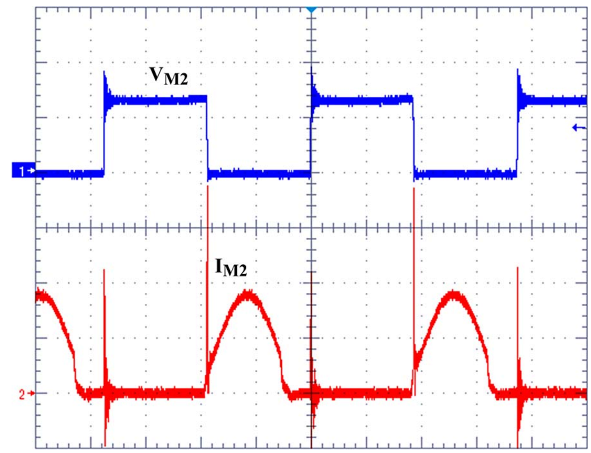

Fig. 10. Voltage (CH1) and current (CH2) waveforms for switch M2 (Ch1: 20 V/div., 2 μs/div.; Ch2:500 mA/div., 2 μs/div.).

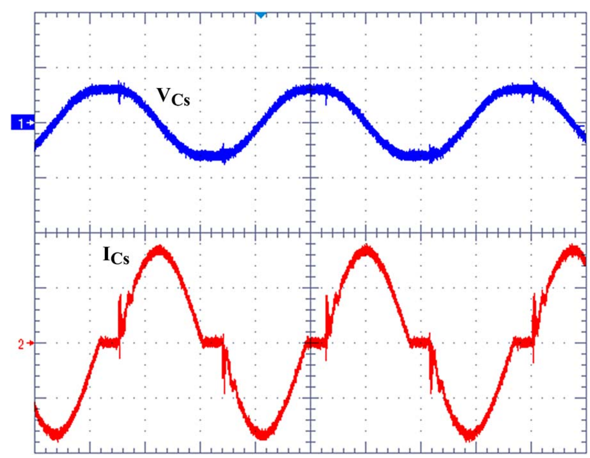

Fig. 11. Voltage (CH1) and current (CH2) waveforms for the SC (Ch1: 10 V/div., 2 μs/div.; Ch2:500 mA/div., 2 μs/div.).

Fig. 11 shows the voltage across and current through the SC. The charge and the discharge of the SC is evidenced, as presented in the theoretical analysis. The rms current through capacitor C_s is about 554.3 mA.

Fig. 12 shows the dependence of the current through the LED on the input voltage. It can be seen that varying the input voltage affects the current through the LED. If the input voltage is reduced e.g., due to the discharging of a battery, the LED brightness will be reduced. Therefore, the input voltage of the converter must remain constant for open loop operation. Otherwise, by using a microcontroller to generate the drive signals of

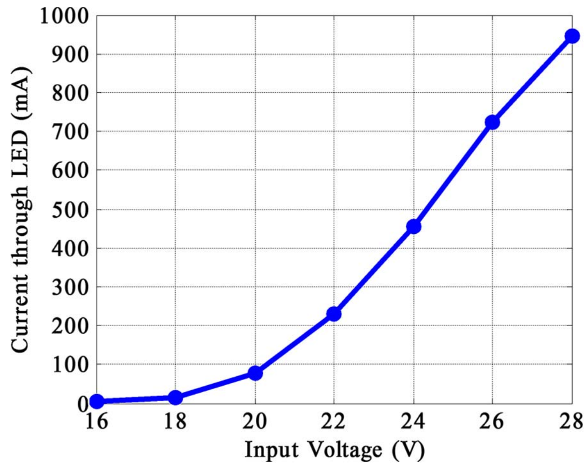

Fig. 12. Current through LEDs versus input voltage.

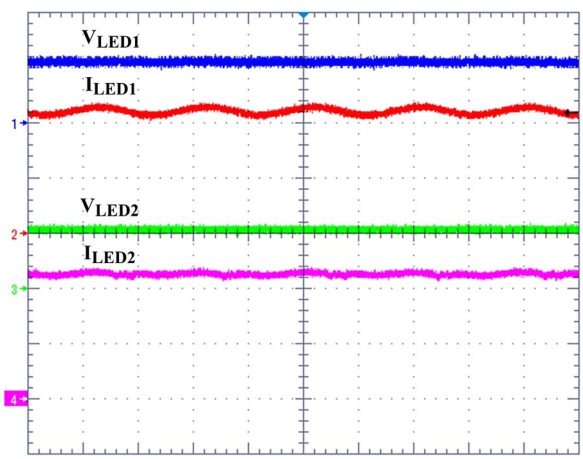

Fig. 13. Voltage (CH1) and current (CH2) through Led Array 1 and voltage (CH3) and current (CH4) through Led Array 2 (Ch1: 10 V/div.; Ch2: 200 mA/div.; Ch3: 10 V/div.; Ch3: 200 mA/div; time base: 2 μs/div.).

the switches, it is possible to adjust the switching frequency to keep the current through the LED array constant when the input voltage varies. For practical applications, the converter should employ frequency modulation to compensate variations of the input voltage. In this paper, a laboratory prototype with open loop control was implemented only to validate the operating principle of the converter.

Fig. 13 shows the voltage and current waveforms for two LED arrays, as depicted in Fig. 6. The second LED array is used in the circuit to show the current sharing among the arrays, each one composed by three series-connected LEDs. Array 1 has an average current of 450.2 mA, average voltage of 10.89 V, which gives a power of 4.90 W. Array 2 has an average current of 452.3 mA and average voltage of 10.63 V, resulting in 4.80 W. Therefore, the total output power is 9.7 W.

Fig. 14 shows the converter efficiency for the operation with one and two LED arrays. To obtain the efficiency plot, the switching frequency was varied to cause the output power to vary. According to (19), reducing the switching frequency causes the output power of the converter to be reduced. In this case, a variable resistor was employed in the oscillator circuit of IC IR2153, so that the switching frequency could be varied.

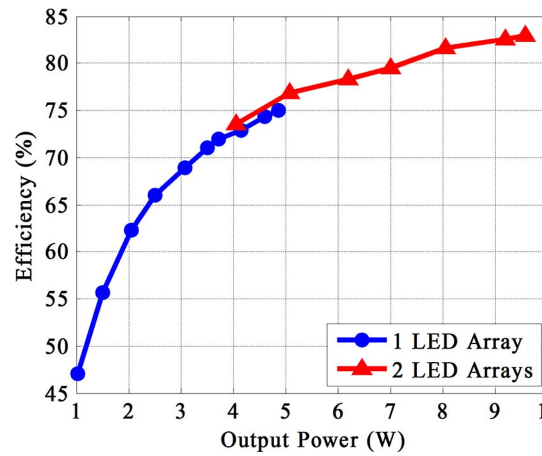

Fig. 14. Converter efficiency as a function of output power.

The same frequency variation was used for operation with one and two LED arrays.

For one LED array, at rated load ($I_{LED} = 457.4$ mA) and switching frequency of 130 kHz, the measured input power is 6.465 W, which corresponds to an efficiency of 75%.

For two LED arrays, rated load and switching frequency of 130 kHz, the measured input power is 11.68 W, which correspond to an efficiency of 83%. With the increase of the power processed by the converter, it can be seen that the efficiency is increased. The losses due to switching operation are independent on the number of LED arrays. Thus, by increasing the load power, the losses caused by the aforementioned intrinsic capacitances are no longer significant. In other words, switching losses tend to become negligible if compared to the total power.

VI. Conclusion

This paper has proposed a LED driver based on a SC converter supplied by a 24 V dc source. The proposed approach differs from traditional SC converters since it uses a small inductor to assist the commutation process of the switches. It has been shown that such inductor does not affect the power transfer to the LED array.

Despite the losses in the MOSFETs, it is possible to replace them for switches with reduced intrinsic capacitances, consequently reducing the turn-on switching losses and making attractive ZCS operation attractive to improve efficiency. To validate the proposed circuit, conventional MOSFETs have been used switches due to wide availability in laboratory.

A 6 W laboratory prototype supplied at 24 V has demonstrated the performance of the proposed topology. The converter operation with one LED array leads to output power of 4.85 W and efficiency of 75%. The converter operating with two LED arrays presented an output power of 9.7 W and efficiency of 83%. By increasing the output power with the addition of more arrays, the converter efficiency tends to increase.

To validate the proposal the converter was implemented in open loop control. However, the power applied to LEDs can be stabilized through the switching frequency as a function of input voltage only. Thus, the converter does not need of current sensors allowing cost reduction.

To future work it is proposed the use of a microcontroller to perform the reading of the input voltage and generate the switching frequency of converter. Thus, it is possible to adjust the switching frequency to keep the LED array current constant toward input voltage variations and also implement the dimming function.

Acknowledgment

The authors express their special thanks to the Energy Processing and Control Group (GPEC), Federal University of Ceará (UFC), and Federal Institute of Ceará (IFCE) where the converter prototype was implemented and evaluated.

References

[1] J. Zhamg, L. Xu, X. Wu, and Z. Qian, "A precise passive current balancing method for multioutput LED srivers," *IEEE Trans. Power Electron.*, vol. 26, no. 8, pp. 2149–2159, Aug. 2011.
[2] V. W. Ng, M. D. Seeman, and S. R. Sanders, "High-efficiency, 12 V-to-1.5 V DC-DC converter realized with switched-capacitor architecture," in *Proc. Symp. VLSI Circuits*, 2009, pp. 168–1699.
[3] T. S. Chong, S. Kiratipongvoot, S. Bronstein, A. Ioinovici, Y. M. Lai, and C. K. Tse, "Adaptive mixed on-time and switching frequency control of a system of interleaved switched-capacitor converters," *IEEE Trans. Power Electron.*, vol. 26, no. 2, pp. 364–380, Feb. 2011.
[4] B. Maity and P. Mandal, "A switched-capacitor based embedded dc-dc buck converter for high power efficiency and high power density," in *Proc. IEEE TENCON*, 2010, pp. 19–24.
[5] O. Keiser, P. K. Steimer, and J. W. Kolar, "High power resonant switched-capacitor step-down converter," in *IEEE PESC*, 2008, pp. 2772–2777.
[6] J. M. Henry and J. W. Kimball, "Practical performance analysis of complex switched-capacitor converters," *IEEE Trans. Power Electron.*, vol. 26, no. 1, pp. 127–136, Jan. 2011.
[7] C.-K. Cheung, S.-C. Tan, Y. M. Lai, and C. K. Tse, "A new visit to an old problem in switched-capacitor converters," in *Proc. IEEE ISCAS*, 2010, pp. 3192–3195.
[8] M. D. Seeman and S. R. Sanders, "Analysis and optimization of switched-capacitor DC-DC Converters," *IEEE Trans. Power Electron.*, vol. 23, no. 2, pp. 841–851, Mar. 2008.
[9] K.-H. Lee *et al.*, "Power-efficient series-charge parallel-discharge charge pump circuit for LED Drive," in *IEEE PESC*, 2008, pp. 2645–2649.
[10] W. Feng and F. G. Shi, "A new switched-capacitor frequency modulated driver for light emitting diodes," *Rev. Sci. Instrum.*, vol. 78, no. 11, pp. 114 701-1–114 701-4, Nov. 2007.
[11] E. M. Sá, Jr., "Estudo de estruturas de reatores eletrônicos para LEDs de iluminação," Ph.D. dissertation, Univ. Federal Santa Catarina, Centro Tecnológico, Santa Catarina, Brazil, 2010.
[12] C. L. Chiu and K. H. Chen, "A high accuracy current-ballanced control technique for LED backlight," in *IEEE PESC*, 2008, pp. 4202–4206.
[13] S. M. Baddela and D. S. Zinger, "Parallel connected LEDs operated at high to improve current sharing," in *Conf. Rec. IEEE IAS Annu. Meeting*, 2004, vol. 3, pp. 1677–1681.
[14] E. M. Sá, Jr., F. L. M. Antunes, and A. J. Perin, "Nova técnica para equalização de corrente em LEDs de alto brilho operando em alta frequência," in *Proc. IEEE INDUSCON-VII*, Recife, Brazil, 2006, pp. 1–6.
[15] J. Zhang, J. Whang, and X. Wu, "A capacitor-isolated LED driver with inherent current balance capability," *IEEE Trans. Ind. Electron.*, vol. 59, no. 4, pp. 1708–1716, Apr. 2012.
[16] J. Wang, J. Zhang, X. Wu, Y. Shi, and Z. Qian, "A novel high efficiency and low-cost current balancing method for multi-LED driver," in *Proc. IEEE ECCE*, 2011, pp. 2296–2301.
[17] K. I. Hwu and S. C. Chou, "A simple current-ballancing converter for LED lighting," in *Proc. IEEE APEC Expo.*, 2009, pp. 587–590.
[18] H. J. Chiu *et al.*, "A high-efficiency dimmable LED driver for low-power lighting applications," *IEEE Trans. Ind. Electron.*, vol. 57, no. 2, pp. 735–743, Feb. 2010.
[19] K. I. Hwu, W. C. Tu, and M. Hong, "A LED current balancing driver with magnetizing inductance energy recycling considered," in *Proc. IEEE APEC Expo.*, 2012, pp. 975–979.
[20] Y. Hu and M. M. Jovanovic, "LED driver with self-adaptive drive voltage," *IEEE Trans. Power Electron.*, vol. 23, no. 6, pp. 3116–3125, Nov. 2008.
[21] A. Zhao and J. C. W. Ng, "An energy conservation based high-efficiency dimmable multi-channel LED driver," in *Proc. IEEE ECCE*, 2011, pp. 2576–2580.
[22] Y.-K. Lo, K.-H. Wu, K.-J. Pai, and H.-J. Chiu, "Design and implementation of RGB LED drivers for LCD backlight modules," *IEEE Trans. Ind. Electron.*, vol. 56, no. 12, pp. 4862–4871, Dec. 2009.
[23] H.-J. Chiu and S.-J. Cheng, "LED backlight driving system for large-scale LCD panels," *IEEE Trans. Ind. Electron.*, vol. 54, no. 5, pp. 2751–2760, Oct. 2007.
[24] K. I. Hwu and Y. T. Yau, "Applying one-comparator counter-based sampling to current sharing control of multi-channel LED string," in *Proc. IEEE APEC Expo.*, 2010, pp. 737–742.
[25] Q. Hu and R. Zane, "LED driver circuit with series-input-connected converter cells operating in continuous conduction mode," *IEEE Trans. Power Electron.*, vol. 25, no. 3, pp. 574–582, Mar. 2010.
[26] S. Choi, P. Agarwal, T. Kim, J. Yang, and B. Han, "Symmetric current balancing circuit for multiple DC loads," in *Proc. IEEE APEC*, 2010, pp. 512–518.
[27] S. Bäurle, D. M. H. Matthews, and R. S. Saint-pierre, "Transformerless safety isolation in a power supply using safety capacitors for galvanic isolation," U.S. Patent 7 453 710, Nov. 18, 2008.
[28] G. Barbehenn and S. B. Elgee, "Sepic converter with transformerless line isolation," U.S. Patent 5 583 421, Dec. 10, 1996.
[29] J. Zhu, M. Xu, J. Sun, and C. Wang, "Novel capacitor-isolated power converter," in *Proc. IEEE Energy Convers. Congr. Expo.*, 2010, pp. 1824–1828.
[30] M. K. Kazimierczuk and D. Czrkoowski, *Resonant Power Converter*, 2nd ed. Hoboken, NJ, USA: Wiley, 2011, pp. 147–150.
[31] P. H. A. Miranda, E. Mineiro Sá, A. V. L. de Oliveira, E. E. dos Santos Filho, and F. L. M. Antunes, "A switched-capacitor driver for power LEDs," in *Proc. COBEP*, 2011, pp. 918–923.
[32] E. Mineiro Sá, Jr., P. H. A. Miranda, E. E. dos Santos Filho, and F. L. M. Antunes, "DC/DC converter with switched capacitor applied for power equalization in LED clusters," *Eletrôn. Potência*, vol. 3, pp. 1100–1108, 2013, (Printed).

Esio Eloi dos Santos Filho (S'12) received the B.Sc. degree in electrical engineering in 2013 from the Federal University of Ceará, Fortaleza, Brazil, where he is currently working toward the M.Sc. degree in electrical engineering.

His current research interests include electronics ballasts, LED lighting, power factor correction circuits, and renewable energy.

Pedro H. A. Miranda received the Technologist degree in industrial mechatronics from the Federal Instiute of Ceará, Fortaleza, Brazil, in 2009, and the M.Sc. degree in electrical engineering from the Federal University of Ceará, Fortaleza, Brazil, in 2012.

He is currently a Professor at the Federal Institute of Ceará, Fortaleza, Brazil, where he coordinates the research department. His research interests include electronic ballasts, microcontrollers, automation, LED lighting, and photovoltaic systems.

Edilson M. Sá, Jr. received the B.S. and M.S. degrees in electrical engineering from the Federal University of Ceará, Fortaleza, Brazil, in 1999 and 2004, respectively, and the Dr. degree from the Federal University of Santa Catarina, Florianopolis, Brazil, in 2010.

Since 2008, he has been a Professor at the Federal Institute of Ceará, Fortaleza, Brazil, where he coordinates the Electronics Laboratory. His research interests include electronic ballasts, power factor correction circuits, dc–dc converters and their application to renewable energy systems, and LED drivers.

Prof. Sá is member of the Brazilian Power Electronics Society-SOBRAEP.

Fernando L. M. Antunes received the B.Sc. degree in electrical engineering from the Federal University of Ceará, Fortaleza, Brazil, in 1978, the B.Sc. degree in business and administration from the State University of Ceará, Brazil, the M.Sc. degree from the University of São Paulo, Butantã, Brazil, and the Ph.D. degree from Loughborough University of Technology, Leicestershire, U.K., in 1991.

In 2006, as a Visiting Professor, he joined the power electronics group of the Fraunhofer IWES (formerly ISET) in Kassel, Germany, to conduct research for designing of multilevel converters for off-shore wind turbines. He is a Professor at the Federal University of Ceará, Fortaleza, Brazil, where he coordinates the power electronics group. His research fields include multilevel converters, inverters, dc–dc converters and their application to renewable energy systems, and LED drivers.

Prof. Antunes is a member of the IEEE Power Electronics and IEEE Industrial Electronics Societies and a member and former President of the Brazilian Power Electronics Society-SOBRAEP.